Local lattice distortions and chemical short-range order in MoNbTaW

A. Fantin[1,2], A.M. Manzoni[1], H. Springer[3], R. Darvishi Kamachali[1], R. Maaß[1,4]

[1]*Federal Institute of Materials Research and Testing (BAM), Unter der Eichen 87, 12205 Berlin, Germany*

[2]*Helmholtz-Zentrum Berlin für Materialien und Energie, Hahn-Meitner-Platz 1, 14019 Berlin, Germany*

[3]*Max-Planck-Institut für Eisenforschung GmbH, Max-Planck-Straße 1, 40237 Düsseldorf, Germany*

[4]*Department of Materials Science and Engineering, University of Illinois at Urbana-Champaign, Urbana, IL 61801, USA*

Supporting Information

Table S1: Estimated diffusion distances x (µm) of all species i in a matrix j for at 2273 K – 24 h. No reliable information exists for the impurity diffusion of W in Ta. Equations of diffusion distances are as follow: $x = \sqrt{Dt}$, with $D = D_0\, exp(-\frac{Q}{RT})$, Q the activity coefficient, R the universal gas constant and T the temperature.

***x* (µm)**		***i***			
		Mo	**Nb**	**Ta**	**W**
j	**Mo**	10-20 [1]	17 [2]	15 [3]	7-10 [3, 4]
	Nb	38 [5]	39-50 [6]	49 [7]	24 [5]
	Ta	14-20 [3, 8, 9]	14-17 [10]	7-16 [6]	-
	W	1 [11]	1 [12]	1 [12, 13]	<1 [6]

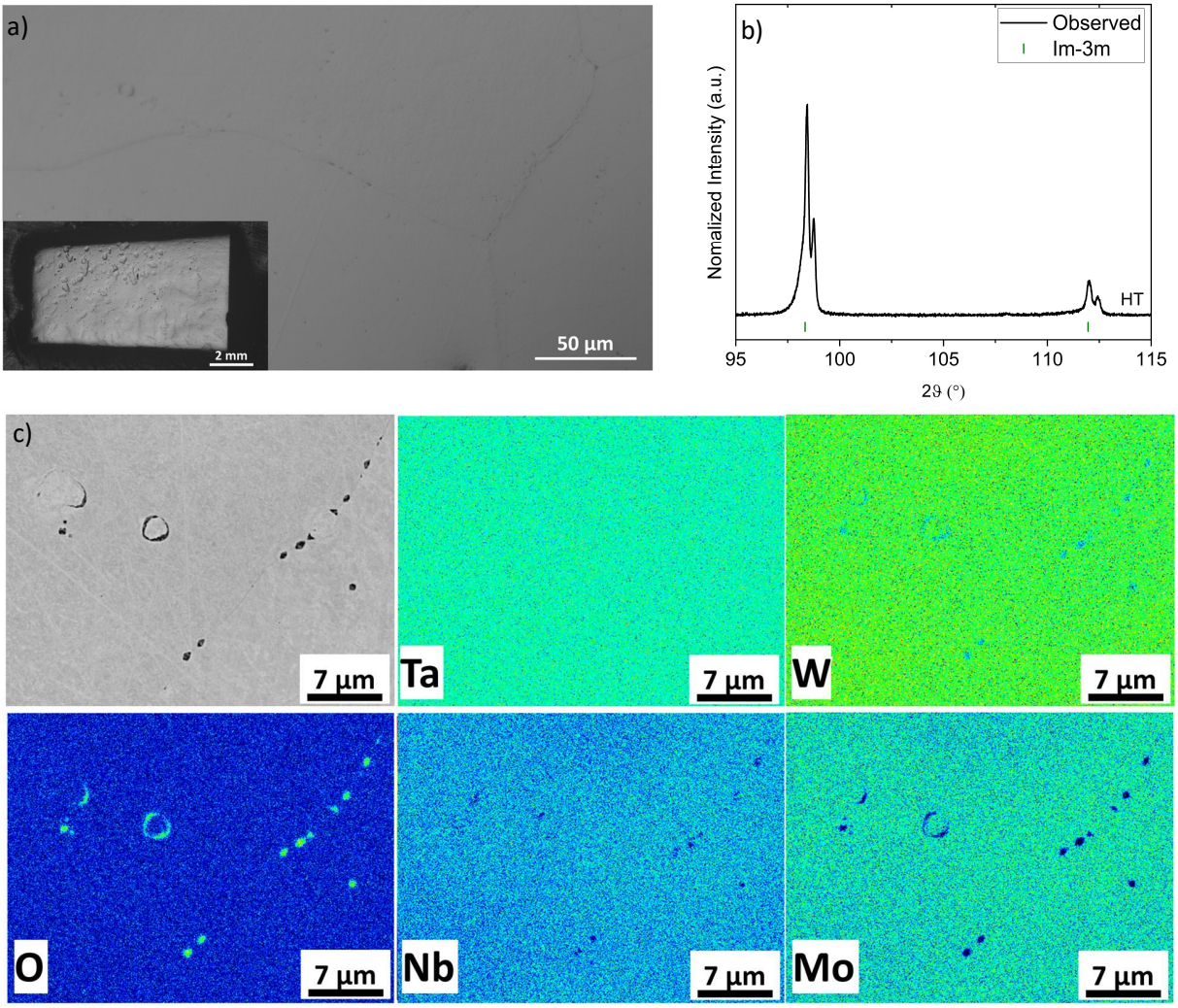

Figure S1. a) optical microscopy showing tiny precipitations at grain boundaries (inset, whole specimen), b) enlargement at high 2Θ (95° ≤ 2Θ ≤ 115°) of the XRD pattern presented in Figure 2, c) BSE image and corresponding EDS maps of the specimen, highlighting small Ta-O enriched zones mainly at the grain boundaries, however not discernable in the X-ray diffraction pattern. Ta-O enriched zones may stem from the heat-treatment: the outer part of the ingot reacted with the ceramic support and some intrusion of oxygen affected the specimen on its outsides.

Table S2. Results from reference foils measured at BM-08 LISA. Amplitude factor reduction S_0^2, fitted energy shift dE_0, shell distances (1st to 5th) are reported together with the uncertainties and the Debye temperature Θ_D accounting for disorder. Notice the extracted metallic radii from the 1st shell distances (half the 1st shell value).

	S_0^2	dE_0(eV)	1st (Å)	Met. radius (Å)	2nd(Å)	3rd(Å)	4th(Å)	5th(Å)	Θ_D (K)
Mo	0.94(5)	3.7(4)	2.719(2)	1.360(1)	3.133(4)	4.445(7)	5.222(7)	5.466(9)	393(16)
Nb	0.95(5)	4.2(3)	2.851(4)	1.425(2)	3.282(5)	4.664(8)	5.492(6)	5.76(1)	293(11)
Ta	0.96(3)	5.1(4)	2.857(2)	1.429(1)	3.290(5)	4.673(7)	5.475(7)	5.81(1)	210(4)
W	0.69(5)	6.2(6)	2.737(2)	1.368(1)	3.159(4)	4.474(6)	5.251(5)	5.487(7)	320(11)

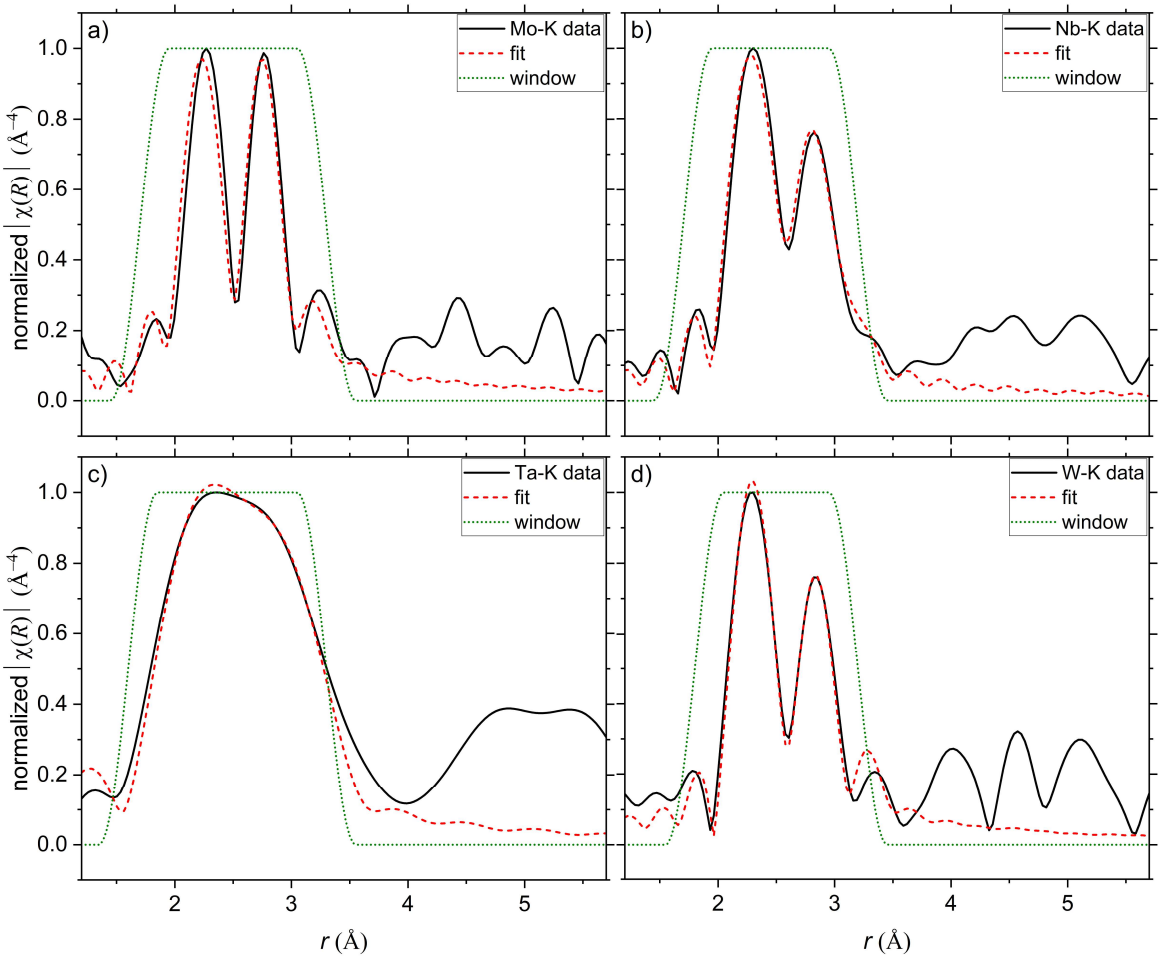

Figure S2. XAS Data fit examples in R*-space at all edges in MoNbTaW: a) Mo K-edge; b) Nb K-edges c) Ta L3-edge; d) W-L3 edge, with* bcc *model as an input. Fitting windows are reported in green. Metallic references fit results are reported in Table S2.*

Table S3: EXAFS fit details for the heat-treated MoNbTaW alloy (top), and corresponding XRD 1st shell and cell parameter obtained experimentally (bottom) for better comparison.

Edge	k range (Å^{-1})	$^{\times}S_0^2$	$^{\times}dE_0$ (eV)	path	NN 1st	NN 2nd	*r* 1st (Å)	*r* 2nd (Å)	θ_D *10^2 (K)
Nb K	3.0-14.5	0.95	4.2	Nb-4*d* Nb-5*d*	4.1(3) 3.9(3)	2.6(5) 3.4(5)	2.786(5) 2.794(7)	3.17(3) 3.16(2)	3.5(3)
Mo K	3.0-14.9	0.94	3.7	Mo-4*d* Mo-5*d*	4.3(4) 3.7(4)	3.5(7) 2.5(7)	2.755(8) 2.76(1)	3.19(2) 3.18(3)	3.3(2)
Ta L$_3$	3.8-8.8*	0.96	5.1	Ta-4*d* Ta-5*d*	*	*	2.77(3) 2.76(4)	3.23(5) 3.21(6)	2.7(9)
W L$_3$	3.0-14.5	0.69	6.2	W-4*d* W-5*d*	4.6(3) 3.4(3)	3.7(4) 2.3(4)	2.770(7) 2.76(2)	3.23(1) 3.23(3)	4.2(7)
XRD (exp)	-	-	-	-	-	-	2.791(1)	3.223(1)	-

Notes: *data quality (cf. main text) did not allow a correct estimate of nearest neighbors. S_0^2: amplitude reduction factor. dE_0: energy shift from threshold. NN and r: nearest neighbors and bond lengths of 1st and 2nd shell, respectively. NN numbers of 4*d* and 5*d* around Ta were set to be equal in the refinements. θ_D: Debye temperature. $^{\times}$ S_0^2 and dE_0 were fixed together on the base of results from pure metal references data.

Table S4. Compositional results (in at. %) from EDX measurements for the as-cast and the heat-treated specimens. Uncertainty (in brackets) represents 1 standard deviation.

	Region	Mo	Nb	Ta	W
As-cast	dendritic	0.232(10)	0.218(11)	0.271(14)	0.279(9)
	interdendritic	0.264(13)	0.273(25)	0.265(16)	0.198(31)
Heat-treated	dendritic	0.226(8)	0.230(9)	0.260(5)	0.284(12)
(2273 K, 24h)	interdendritic	0.246(2)	0.264(4)	0.258(2)	0.232(5)

Table S5: Reference lattice parameters a and metallic radii obtained in pure metals from Refs. [14, 15] are shown together with extracted metallic radii from XAS fitting of pure metal references (cf. S.I. for fitting details). Therefore, the depicted metallic radii refer to 8-coordination symmetry. In addition, calculated 1st and 2nd nearest neighbor (NN) distances according to Vegard's law using tabulated and XAS extracted metallic radii, together with experimentally determined 1st and 2nd NN distances from conventional X-ray diffraction.

Composition	Method	Lattice a (XRD) (Å, 298 K)	Met. radii (XRD), $\frac{\sqrt{3}}{4}a$	Met. radii (XAS)
Nb	XRD, XAS	3.3007 [15]	1.4292	1.425(2)
Mo	XRD, XAS	3.1410 [14]	1.3601	1.360(1)
Ta	XRD, XAS	3.3019 [15]	1.4298	1.429(1)
W	XRD, XAS	3.1583 [14]	1.3676	1.368(1)
MoNbTaW	**Vegard (1st NN)**	2.793		2.791(2)
	Vegard (2nd NN)	3.225		3.223(3)
MoNbTaW	**XRD (1st NN)**	2.791(1)		
	XRD (2nd NN)	3.223(1)		

References

[1] K. Maier, H. Mehrer, G. Rein, Self-Diffusion in Molybdenum, International Journal of Materials Research 70(4) (1979) 271-276.
[2] G.B. Fedorov, E.A. Smirnov, V.N. Gusev, F.I. Zhomov, V.L. Gorbenko, Met. Metalloved. Chist. Met. 10 (1973).
[3] F. Roux, Contribution à l'étude des phénomènes de diffusion dans le niobium et le molybdène, Université de Nancy I, Nancy, 1972.
[4] W. Erley, H. Wagner, The diffusion coefficients in the system molybdenum–tungsten, physica status solidi (a) 25(2) (1974) 463-471.
[5] F. Roux, A. Vignes, Diffusion dans les systèmes Ti-Nb, Zr-Nb, V-Nb, Mo-Nb, W-Nb, Rev. Phys. Appl. (Paris) 5(3) (1970) 393 - 405.
[6] G. Neumann, V. Tölle, Self-diffusion in body-centred cubic metals: Analysis of experimental data, Philosophical Magazine A 61(4) (1990) 563-578.
[7] T.S. Lundy, F.R. Winslow, R.E. Pawel, C.J. McHargue, Diffusion of Nb-95 and Ta-182 in Niobium (Columbium), Trans. Met. Soc. AIME 233 (1965).
[8] F. Guillemot, M. Boliveau, M. Bohn, J. Debuigne, D. Ansel, On the diffusion in the Mo–Ta refractory system, International Journal of Refractory Metals and Hard Materials 19(3) (2001) 183-189.
[9] E.V. Borisov, P.L. Gruzin, S.V. Zemskii, Zash. Pokryt. Met. 2 (1968).
[10] G. Neumann, V. Tölle, Impurity Diffusion in Body-Centred Cubic Metals: Analysis of Experimental Data, International Journal of Materials Research 82(10) (1991) 741-744.
[11] S.M. Klotsman, V. Koloskov, S. Osetrov, I. Polikarpova, G. Tatarinova, A. Timofeev, Diffusion of chromium and molybdenum in tungsten single crystals (in Russian), Fiz. Met. Metalloved. 67 (1989).
[12] R.E. Pawel, T.S. Lundy, Tracer diffusion in tungsten, Acta Metallurgica 17(8) (1969) 979-988.
[13] N.K. Arkhipova, S.M. Klotsman, I.P. Polikarpova, G.N. Tatarinova, A.N. Timofeev, L.M. Veretennikov, Tungsten-series impurity diffusion in single-crystal tungsten, Phys Rev B 30(4) (1984) 1788-1796.

[14] E.R. Jette, F. Foote, Precision Determination of Lattice Constants, The Journal of Chemical Physics 3(10) (1935) 605-616.
[15] Y.M. Smirnov, V. Finkel, Crystal Structure of Tantalum, Niobium, and Vanadium at 110-400°K, Journal of Experimental and Theoretical Physics 22 (1966) 750.